

## Supplemental Material

### Tetra (C<sub>60</sub>) lanthanum phthalocyanine: design, synthesis and investigation of third-order nonlinear optical properties.

Min Zhu, Jiale Ding, Sen Niu, Yunhe Zhang\*, Guibin Wang

*Key Laboratory of High Performance Plastics (Jilin University) Ministry of Education, College of Chemistry, Jilin University, Changchun, 130012, P. R. China*

#### 1. Characterisation of monomer 1

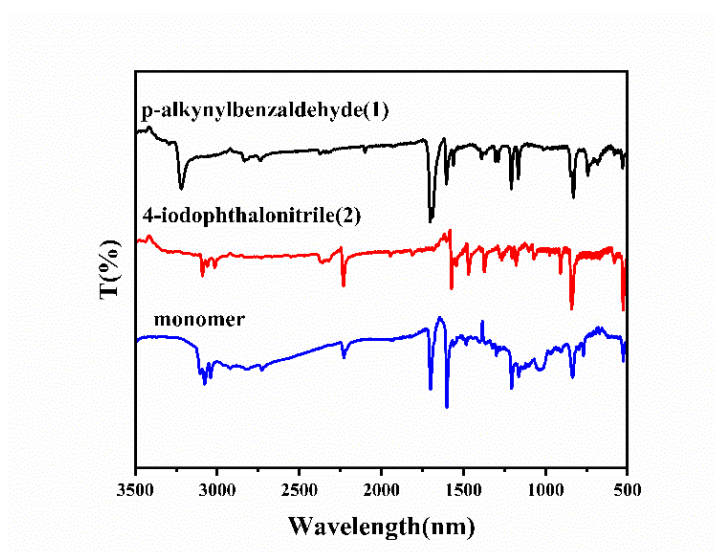


**Fig. S1.** FT-IR spectra of compounds (1), (2) and monomer.

The infrared spectra of (1), (2) and the monomer 1 are shown in Fig. S1. In the spectrum of the monomer 1, it can be seen that the vibrational absorption peak of CN is at 2230 cm<sup>-1</sup>, and the stretching vibration absorption peak of C-H is near 1090 cm<sup>-1</sup>; The peak around 660-900 cm<sup>-1</sup> corresponds to the out-of-plane bending vibration of the phenyl C-C bond; and the peak at 1742 cm<sup>-1</sup> corresponds to the stretching vibration of the C=O bond.

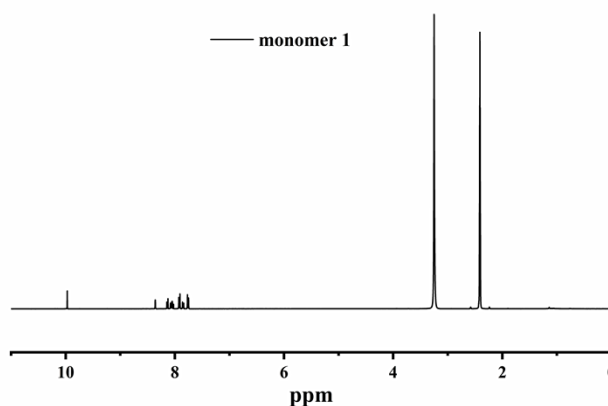


**Fig. S2.** <sup>1</sup>H NMR spectra of monomer 1.

The <sup>1</sup>H NMR spectra of monomer 1 is shown in Fig. S2. It exhibited the bands at approximately 7.85-8.49 ppm and 10.00 ppm, which were attributed to the H of Benzene and H of Aldehyde group. All the above results provide evidence of that monomer 1 has been successfully synthesized.

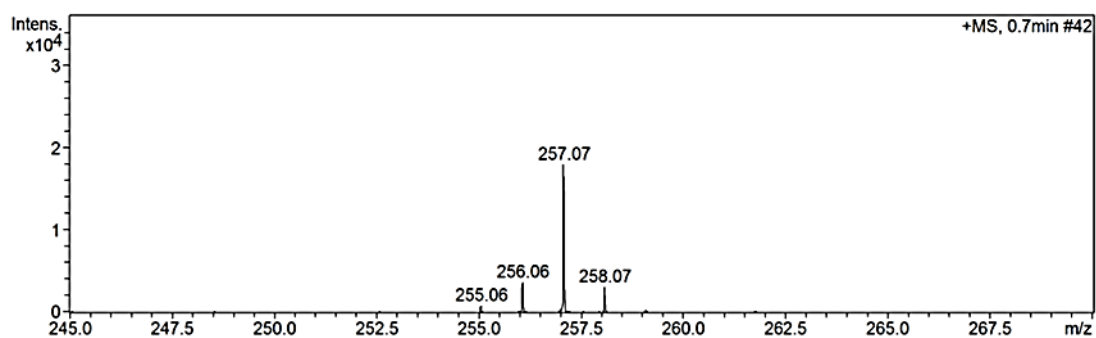


**Fig S3.** The high resolution mass spectrum of monomer 1

2. <sup>1</sup>H NMR spectra and MALDI-TOF-MS spectra of LaPc

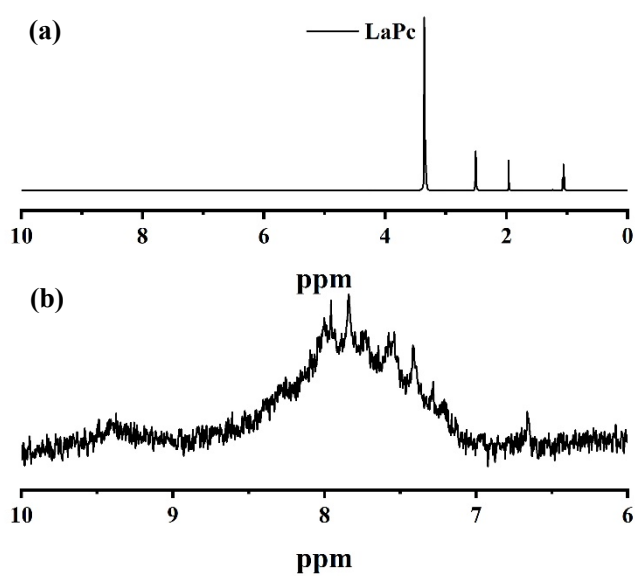


**Fig. S4.** (a) <sup>1</sup>H NMR spectra of LaPc; (b) the partial enlarged <sup>1</sup>H NMR spectra of LaPc.

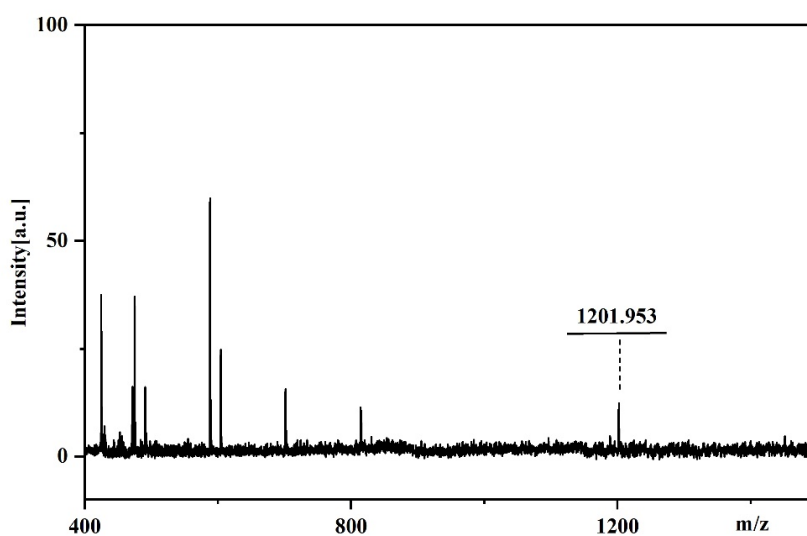


**Fig S5.** The MALDI-TOF-MS spectra of LaPc is shown in Fig S5.

3.  $^1\text{H}$  NMR spectra and MALDI-TOF-MS spectra of tetra ( $\text{C}_{60}$ )-LaPc

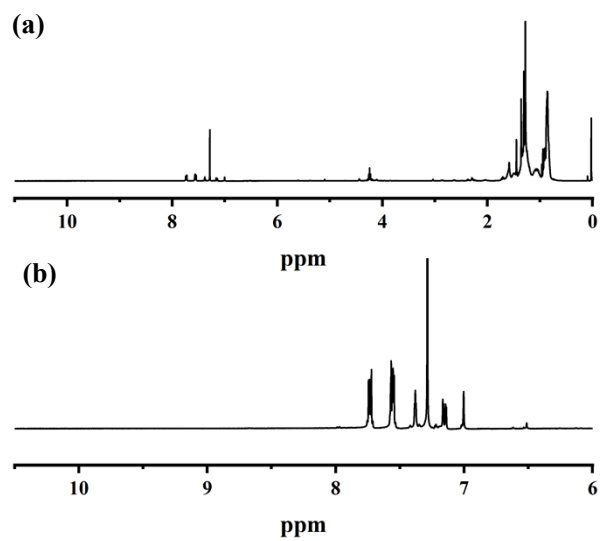


**Fig S6.**  $^1\text{H}$  NMR spectra of tetra ( $\text{C}_{60}$ )-LaPc with Chloroform-d ( $\text{CDCl}_3$ ) as the solvent.

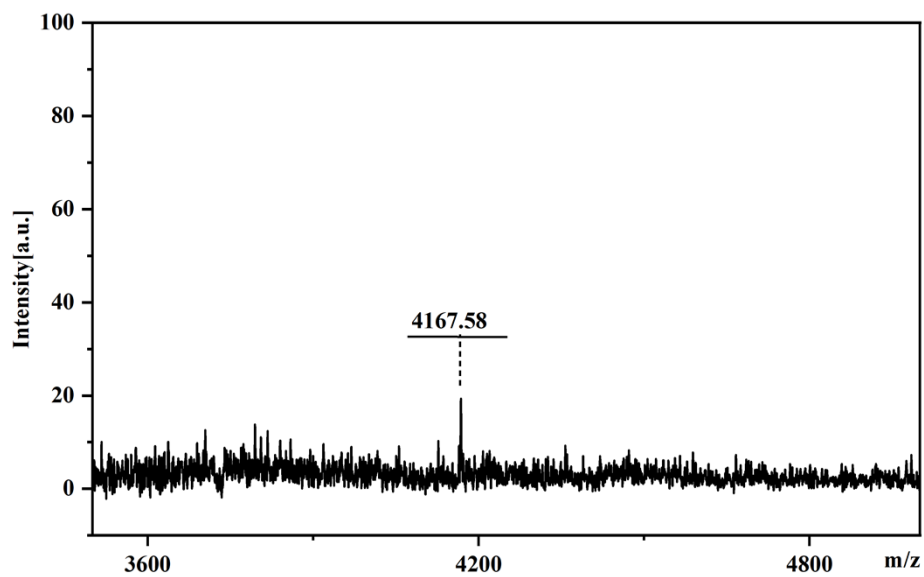


**Fig S7.** The MALDI-TOF-MS spectra of tetra ( $\text{C}_{60}$ )-LaPc is shown in Fig S5.

#### 4. XPS spectra

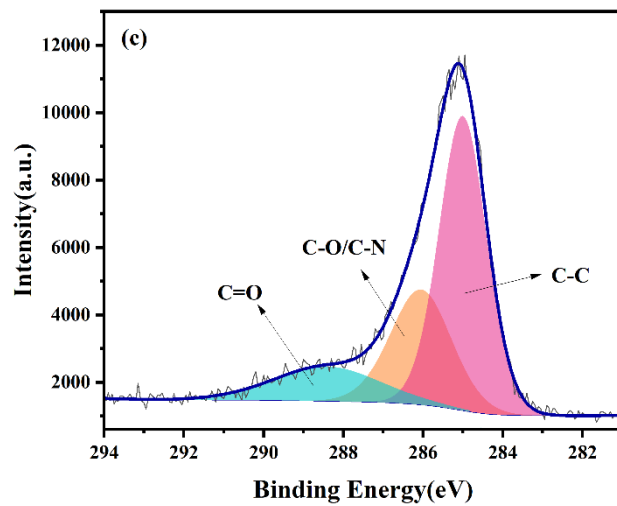


Fig. S8. XPS spectra of C 1s of LaPc.

#### 5. Tauc spectra

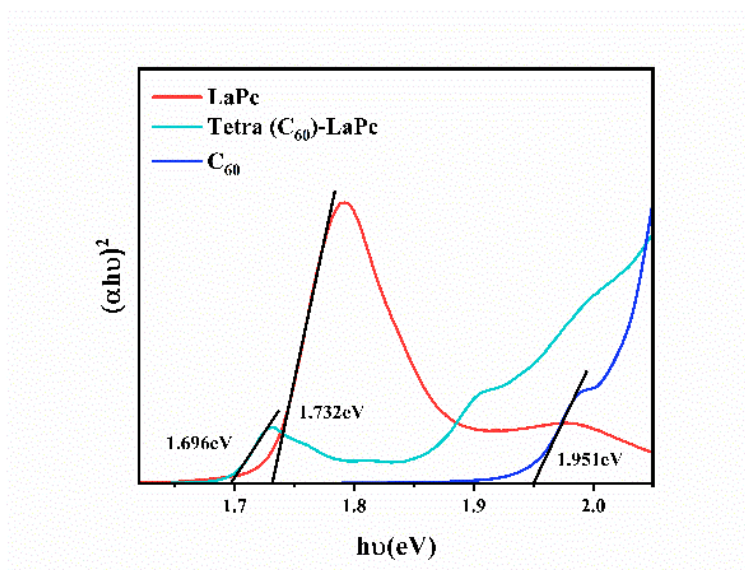
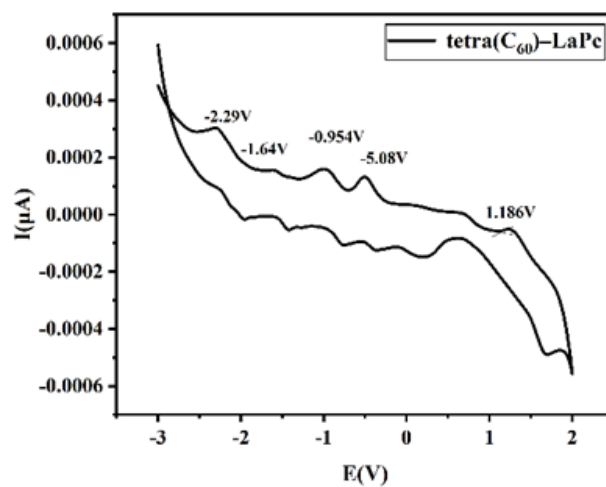


Fig. S9. Tauc spectra of C<sub>60</sub>, LaPc and tetra (C<sub>60</sub>)-LaPc.

## 6. CV spectra



**Fig S10.** The CV spectra of tetra(C<sub>60</sub>)-LaPc.

**Table S1.** E<sub>g</sub>, LUMO Energy Levels of the samples.

Samples	E <sub>LUMO</sub> (eV)	E <sub>g</sub> (eV)	λ <sub>max</sub> (1)	λ <sub>max</sub> (2)
LaPc	-3.275	1.732	693	705
C <sub>60</sub>	-3.304	1.951	/	/
tetra(C <sub>60</sub> )-LaPc	-3.792	1.696	705	710

λ<sub>max</sub> (1) is the maximum absorption peak in the UV-Q band; λ<sub>max</sub>(2) is the maximum fluorescence emission peak.

## 7. UV-vis absorption and fluorescence emission spectra

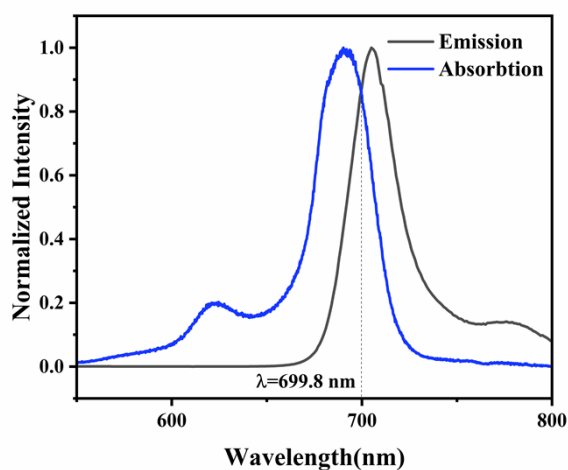


**Fig. S11.** The normalized curves (a) UV-vis absorption and fluorescence emission spectra.

## 8. Z-scan spectra

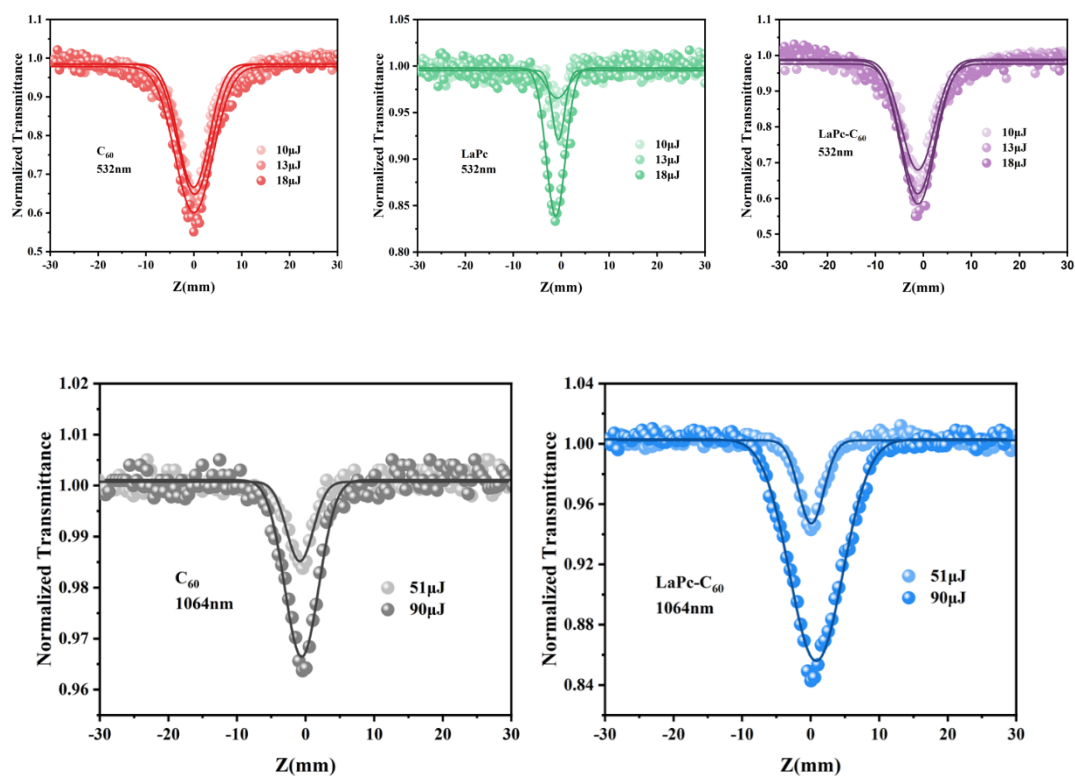


**Fig S12.** Open-aperture Z-scan curves of C<sub>60</sub>, LaPc and tetra(C<sub>60</sub>)–LaPc nm excited by the different input energies at 532 nm and at 1064 nm with similar linear transmittance.

The changes in the curve of Z-scan at different incident light intensities have been shown in Fig. S11. The third-order non-linear optical intensities of C<sub>60</sub>, LaPc and tetra(C<sub>60</sub>)–LaPc increase with the growing incident laser intensity, and in particular the anti-saturation absorption of tetra(C<sub>60</sub>)–LaPc is significantly enhanced, which can be attributed to its effective intramolecular PET/ET process.